



Stress concentration around a hole in a radially inhomogeneous plate

Mohsen Mohammadi^{*}, John R. Dryden, Liyang Jiang

Department of Mechanical and Materials Engineering, The University of Western Ontario, London, Ontario, Canada N6A 5B9

ARTICLE INFO

Article history:

Received 25 March 2010
Received in revised form 27 September 2010
Available online 20 October 2010

Keywords:

Functionally graded materials
Stress concentration factor
Circular hole
Biaxial tension
Pure shear loading

ABSTRACT

The stress concentration factor around a circular hole in an infinite plate subjected to uniform biaxial tension and pure shear is considered. The plate is made of a functionally graded material where both Young's modulus and Poisson's ratio vary in the radial direction. For plane stress conditions, the governing differential equation for the stress function is derived and solved. A general form for the stress concentration factor in case of biaxial tension is presented. Using a Frobenius series solution, the stress concentration factor is calculated for pure shear case. The stress concentration factor for uniaxial tension is then obtained by superposition of these two modes. The effect of nonhomogeneous stiffness and varying Poisson's ratio upon the stress concentration factors are analyzed. A reasonable approximation in the practical range of Young's modulus is obtained for the stress concentration factor in pure shear loading.

© 2010 Elsevier Ltd. All rights reserved.

1. Introduction

Functionally graded materials (FGMs) were initially brought to scientific attention in 1984 (Koizumi, 1997). These nonhomogeneous composites are used in various applications (see, e.g. Watari et al., 1997; Simonet et al., 2007). The composition and the morphology of FGMs gradually change over the volume; consequently, the elastic properties of the material change with position (Miyamoto et al., 1999). Of particular interest in this contribution is the special case where the elastic properties within an elastic body vary in the radial direction but are independent of tangential direction. This type of inhomogeneity can be due to several causes: directional cooling leading to a microstructural gradient (Markworth et al., 1995); phase segregation arising as a result of centrifugal casting (Fukui et al., 1999); and surface modification using laser technology (Islam, 1996).

The elastic stress field in FGMs, where the elastic properties vary in the radial direction, has recently received considerable attention (Horgan and Chan, 1999; Noda, 1999; Zimmerman and Lutz, 1999; Dryden and Jayaraman, 2006). For these types of FGMs most of the analytic investigation has been axisymmetric and directed toward pressurized FG tubes and disks (Tutuncu, 2007; Mohammadi and Dryden, 2009), curved beams (Kardomateas, 1990; Dryden, 2007; Mohammadi and Dryden, 2008), and thermal stress analysis (Jabbari et al., 2002; Lutz and Zimmerman, 1996a).

There has been less analytical investigation on the effect of radial inhomogeneity upon the elastic field in non-axisymmetric problems (see, e.g. Batra and Nie, 2009; Nie and Batra, 2009).

Curved beams have been investigated by Lekhnitskii (1981). Other geometries such as hollow cylinders by Shao et al. (2008), spheres by Poultangari et al. (2008), pressurized vessels by Jabbari et al. (2003), and spherical inclusions by Lutz and Zimmerman (1996b). In most of these contributions power law functions have been used to define the variation of elastic properties. Here we want to calculate the stress field around a circular hole subjected to uniform far-field stress and power law functions are not suitable to define the spatial variation of Young's modulus in an infinite plate.

The stress concentration factor around a hole in a homogeneous plate has been received much attention over the last two centuries (see, e.g. Savin, 1961; Pilkey and Pilkey, 2008). In the case of functionally graded materials, some numerical work has been done recently. Using an isoparametric finite element formulation, Kubair and Bhanu-Chandar (2008) investigated stress concentration around a circular hole in functionally graded panels under uniaxial tension. They found that the stress concentration factor is reduced when Young's modulus progressively decreases towards the hole. Subsequently, Yang et al. (2009) investigated the stress field around a circular hole in a FGM plate. They used piece-wise homogeneous layers and complex variable methods. The plate was decomposed into N rings with equal thickness and constant material properties. The elastic fields for different spatial variations of the elastic properties were calculated.

The aim of this contribution is to present an analytical calculation for the stress concentration factor around a circular hole in an infinite plate made of an inhomogeneous material subjected to uniform biaxial tension and pure shear loading. Here, both Young's modulus and Poisson's ratio are smooth monotonic functions of the radius and attain limiting values far from the hole. Exponential

^{*} Corresponding author. Tel.: +1 519 611 2111x80215; fax: +1 519 661 3020.
E-mail address: mmoham29@uwo.ca (M. Mohammadi).

functions are used to define the variation of elastic properties. A closed form expression for the stress concentration factor for biaxial tension is presented; the expression for the stress concentration factor for pure shear loading is obtained in terms of series solution. The influence of nonhomogeneous stiffness and varying Poisson's ratio on the stress concentration factor for both cases are then considered. Finally, an approximation for the stress concentration factor for pure shear loading is obtained.

2. Description of the inhomogeneity

Consider an infinite plate with a circular hole of radius a where the plate is subjected to a uniform far-field stress. The presence of the hole changes the elastic field in the vicinity of the hole and to calculate the stress, polar coordinates are used. The radial coordinate, r , is normalized with respect to the radius of the hole, and a dimensionless radius is then defined as $\rho = r/a$. The elastic solid is nonhomogeneous, but here it is considered to be isotropic. The material properties change in the radial direction and approach uniform values at distances far away from the hole. As described in Section 1, this type of nonhomogeneity can be due to several reasons. With this behavior in mind, a dimensionless function $\kappa(\rho)$ is introduced and Young's modulus E is written as

$$E = E_\infty \kappa(\rho). \quad (1)$$

Similarly, Poisson's ratio is expressed as

$$\nu = \nu_0 + (\nu_\infty - \nu_0)\kappa(\rho). \quad (2)$$

There are many functions that can be used to describe the behavior of κ and here the only restrictions are that

$$\kappa(\infty) = 1, \quad \kappa_1 \equiv \frac{E_1}{E_\infty} \equiv \kappa(1) > 0. \quad (3)$$

At large distances from the hole $E = E_\infty$ and $\nu = \nu_\infty$; whereas at the periphery of the hole, $E_1 = E_\infty \kappa_1$ and $\nu_1 = \nu_0 + (\nu_\infty - \nu_0)\kappa_1$. The parameter ν_0 is adjustable.

3. Governing differential equation

Suppose that the plate is subjected to a uniform far-field stress. Near the hole the uniform elastic field is perturbed and a polar coordinate system is used to calculate the stresses. The basic elastic equations for plane stress are given. First, the displacement components U and V , in the radial and tangential directions respectively, are normalized, $u = U/a$ and $v = V/a$. The strain-displacement relations are well known (see, for example Timoshenko and Goodier, 1970), and the relevant terms are

$$\epsilon_\rho = \frac{\partial u}{\partial \rho}, \quad (4)$$

$$\epsilon_\theta = \frac{u}{\rho} + \frac{1}{\rho} \frac{\partial v}{\partial \theta}, \quad (5)$$

$$\gamma_{\rho\theta} = \frac{\partial v}{\partial \rho} - \frac{v}{\rho} + \frac{1}{\rho} \frac{\partial u}{\partial \theta}, \quad (6)$$

where ϵ_ρ , ϵ_θ , and $\gamma_{\rho\theta}$ represent the normal and shear strain components, respectively. The compatibility equation is given in reference Wang (1953) and is written as

$$\frac{\partial}{\partial \rho} \left(\frac{\partial(\rho \epsilon_\theta)}{\partial \rho} - \epsilon_\rho \right) + \frac{1}{\rho} \frac{\partial^2 \epsilon_\rho}{\partial \theta^2} = \frac{1}{\rho} \frac{\partial}{\partial \theta} \left(\frac{\partial \gamma_{\rho\theta}}{\partial \rho} + \frac{\gamma_{\rho\theta}}{\rho} \right). \quad (7)$$

The normal and shear stresses are labeled as σ_ρ , σ_θ , and $\tau_{\rho\theta}$, respectively. The two equilibrium equations are given by Timoshenko and Goodier (1970):

$$\rho\text{-direction: } \frac{\partial \sigma_\rho}{\partial \rho} + \frac{1}{\rho} \frac{\partial \tau_{\rho\theta}}{\partial \theta} + \frac{\sigma_\rho - \sigma_\theta}{\rho} = 0, \quad (8)$$

$$\theta\text{-direction: } \frac{1}{\rho} \frac{\partial \sigma_\theta}{\partial \theta} + \frac{\partial \tau_{\rho\theta}}{\partial \rho} + \frac{2\tau_{\rho\theta}}{\rho} = 0. \quad (9)$$

The solid is a linear elastic material and in plane stress; Hooke's law is written as

$$\epsilon_\rho = \frac{1}{E} (\sigma_\rho - \nu \sigma_\theta), \quad (10)$$

$$\epsilon_\theta = \frac{1}{E} (\sigma_\theta - \nu \sigma_\rho), \quad (11)$$

$$\gamma_{\rho\theta} = \frac{2(1+\nu)}{E} \tau_{\rho\theta}, \quad (12)$$

where E and ν are defined by Eqs. (1) and (2), respectively. It is noted that, the average values of displacement, strain, and stress across the thickness are used in this study and for the sake of simplicity the overbar is omitted from all of these average values (Love, 1906).

If $\psi(\rho, \theta)$ is the stress function, then the stress components are given by

$$\sigma_\rho = \frac{1}{\rho} \frac{\partial \psi}{\partial \rho} + \frac{1}{\rho^2} \frac{\partial^2 \psi}{\partial \theta^2}, \quad (13)$$

$$\sigma_\theta = \frac{\partial^2 \psi}{\partial \rho^2}, \quad (14)$$

$$\tau_{\rho\theta} = \frac{1}{\rho^2} \frac{\partial \psi}{\partial \theta} - \frac{1}{\rho} \frac{\partial^2 \psi}{\partial \rho \partial \theta}. \quad (15)$$

It is well known that the stress components defined in this way satisfy the equilibrium equations (Wang, 1953). Combining the above equations, the strain can be written in terms of the stress function:

$$E_\infty \epsilon_\rho = \frac{1}{\kappa} \left(\frac{1}{\rho} \frac{\partial \psi}{\partial \rho} + \frac{1}{\rho^2} \frac{\partial^2 \psi}{\partial \theta^2} - \nu_0 \frac{\partial^2 \psi}{\partial \rho^2} \right) - (\nu_\infty - \nu_0) \left(\frac{\partial^2 \psi}{\partial \rho^2} \right), \quad (16)$$

$$E_\infty \epsilon_\theta = \frac{1}{\kappa} \left(\frac{\partial^2 \psi}{\partial \rho^2} - \frac{\nu_0}{\rho} \frac{\partial \psi}{\partial \rho} - \frac{\nu_0}{\rho^2} \frac{\partial^2 \psi}{\partial \theta^2} \right) - (\nu_\infty - \nu_0) \left(\frac{1}{\rho} \frac{\partial \psi}{\partial \rho} + \frac{1}{\rho^2} \frac{\partial^2 \psi}{\partial \theta^2} \right), \quad (17)$$

$$E_\infty \gamma_{\rho\theta} = \frac{2(1+\nu_0)}{\kappa} \left(\frac{1}{\rho^2} \frac{\partial \psi}{\partial \theta} - \frac{1}{\rho} \frac{\partial^2 \psi}{\partial \rho \partial \theta} \right) + 2(\nu_\infty - \nu_0) \left(\frac{1}{\rho^2} \frac{\partial \psi}{\partial \theta} - \frac{1}{\rho} \frac{\partial^2 \psi}{\partial \rho \partial \theta} \right), \quad (18)$$

where κ , ν_0 , and ν_∞ are defined in Eqs. (1) and (2). By inserting Eqs. (16)–(18) into the compatibility condition (7), the governing partial differential equation for the stress function is obtained:

$$\nabla^2 \nabla^2 \psi - \frac{\kappa'}{\kappa} \left\{ 2 \frac{\partial^3 \psi}{\partial \rho^3} + \left(\frac{2-\nu_0}{\rho} \right) \frac{\partial^2 \psi}{\partial \rho^2} - \frac{1}{\rho^2} \frac{\partial \psi}{\partial \rho} - \frac{3}{\rho^3} \frac{\partial^2 \psi}{\partial \theta^2} + \frac{2}{\rho^2} \frac{\partial^3 \psi}{\partial \theta^2 \partial \rho} \right\} + \frac{2\kappa'^2 - \kappa''\kappa}{\kappa^2} \left\{ \frac{\partial^2 \psi}{\partial \rho^2} - \frac{\nu_0}{\rho} \frac{\partial \psi}{\partial \rho} - \frac{\nu_0}{\rho^2} \frac{\partial^2 \psi}{\partial \theta^2} \right\} = 0, \quad (19)$$

where ' and '' are the first and second total derivatives with respect to ρ . The biharmonic equation $\nabla^2 \nabla^2 \psi$ is defined by

$$\nabla^2 \nabla^2 \psi = \left(\frac{\partial^2}{\partial \rho^2} + \frac{1}{\rho} \frac{\partial}{\partial \rho} + \frac{1}{\rho^2} \frac{\partial^2}{\partial \theta^2} \right) \left(\frac{\partial^2 \psi}{\partial \rho^2} + \frac{1}{\rho} \frac{\partial \psi}{\partial \rho} + \frac{1}{\rho^2} \frac{\partial^2 \psi}{\partial \theta^2} \right). \quad (20)$$

For the case of homogeneous materials, κ is constant and Eq. (19) reduces to $\nabla^2 \nabla^2 \psi = 0$, (see, for example Timoshenko and Goodier, 1970; Love, 1906). It is noted that the terms involving $v_\infty - v_0$ do not enter into the final governing differential Eq. (19) and the stress function only depends on v_0 .

3.1. The general form of the stress function

The stress function ψ is assigned the separable form

$$\psi(\rho, \theta) = f(\rho) \cos(m\theta) \quad (21)$$

and upon substituting this into Eq. (19), the governing equation reduces to an ordinary differential equation which is

$$\rho^4 f'''' + \rho^3 [2 - 2g] f''' + \rho^2 [g(v_0 - 2) + h - 1 - 2m^2] f'' + \rho [(g + 1)(1 + 2m^2) - hv_0] f' + [m^4 + m^2(hv_0 - 3g - 4)] f = 0, \quad (22)$$

where g and h are dimensionless functions that describe the nonhomogeneity:

$$g = \frac{\rho \kappa'}{\kappa}, \quad (23)$$

$$h = g^2 + g - g' \rho. \quad (24)$$

Here we want to calculate the stress concentration factor around a hole subjected to: (1) biaxial loading, $m = 0$, as shown in Fig. 1(a), and (2) pure shear, $m = 2$, as shown in Fig. 1(b). The former is an axisymmetric problem, while the latter is non-axisymmetric.

4. Stress state due to biaxial tension: $m = 0$

Consider the far-field stress corresponding to $m = 0$ as shown in Fig. 1(a). The governing differential Eq. (22) becomes

$$\rho^4 f'''' + 2\rho^3 [1 - g] f''' + \rho^2 [g(v_0 - 2) + h - 1] f'' + \rho [g + 1 - hv_0] f' = 0 \quad (25)$$

and this represents an axisymmetric stress field. After some algebra, it can be verified that Eq. (25) can be written as

$$\left[\frac{\rho}{\kappa} \left\{ f''' + \left(\frac{1-g}{\rho} \right) f'' - \left(\frac{1-v_0 g}{\rho^2} \right) f' \right\} \right]' = 0. \quad (26)$$

Defining $p \equiv f$, the governing differential equation is then reduced to

$$p'' + \left(\frac{1-g}{\rho} \right) p' - \left(\frac{1-v_0 g}{\rho^2} \right) p = \frac{\varepsilon \kappa}{\rho}, \quad (27)$$

where the coefficient ε is the constant of integration. The particular solution of Eq. (27) associated with the constant ε corresponds to the bending problem and is not required here.

The periphery of the hole is stress free and the radial stress is equal to σ_0 at infinity; therefore, the boundary conditions for this problem are

$$p(1) = 0, \quad \lim_{\rho \rightarrow \infty} \frac{p}{\rho} = \sigma_0. \quad (28)$$

Suppose that p_1 and p_2 are two linearly independent solutions of Eq. (27) where the constant ε is set equal to zero. Considering the boundary conditions (28), the stress function p is written as

$$p = \sigma_0 \left(\frac{p_1(\rho) p_2(1) - p_2(\rho) p_1(1)}{p_2(1)} \right). \quad (29)$$

The stress concentration factor, K_0 , corresponding to hydrostatic loading can be found from this stress function.

The factor K_0 is defined as the ratio of the maximum hoop stress which occurs at $\rho = 1$ to the reference stress σ_0 (Pilkey and Pilkey, 2008). Using Eqs. (14) and (29), it follows that

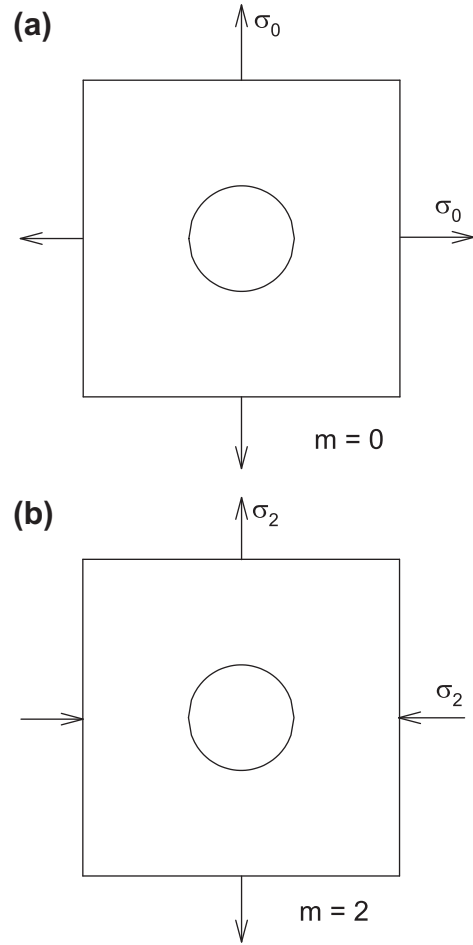


Fig. 1. Far-field loading on the plate containing the circular hole: (a) shows the biaxial loading σ_0 , corresponding to $m = 0$; and (b) shows pure shear σ_2 , corresponding to $m = 2$.

$$K_0 = \frac{p'_1(1)p_2(1) - p'_2(1)p_1(1)}{p_2(1)}. \quad (30)$$

The numerator of Eq. (30) is equal to the Wronskian evaluated at $\rho = 1$, (see, for example Braun, 1993). In this case the Wronskian, $W = p'_1 p_2 - p'_2 p_1 = C \kappa(\rho)/\rho$ where $\kappa(\rho)$ is defined in Eq. (1). The elastic properties become uniform at large distances away from the hole, i.e. $\kappa(\infty) = 1$, so that the solutions must be such that $p_1 \sim \rho$ and $p_2 \sim 1/\rho$. It then follows that the constant $C = 2$ and the Wronskian can be written as $W = 2\kappa(\rho)/\rho$. The stress concentration factor is then expressed as

$$K_0 = 2 \left(\frac{E_1}{E_\infty} \right) \Sigma_0, \quad (31)$$

where the normalized stress concentration factor Σ_0 is

$$\Sigma_0 = \frac{1}{p_2(1)}. \quad (32)$$

It is noted that, Σ_0 is a function of s , v_0 , and E_1/E_∞ . In order to obtain an analytical expression for K_0 , a definite form must be assigned to the function $\kappa(\rho)$.

4.1. Spatial variation of $\kappa(\rho)$

For the kind of inhomogeneity envisaged in this paper there are two main features. First, there is the value of the stiffness at the hole periphery, and secondly, there is the rate at which the

inhomogeneity decays away from the hole. These two features can be captured by the following expression:

$$\kappa(\rho) = \exp(x), \quad \text{where } x = \eta\rho^s, \quad (33)$$

where η and $s < 0$ are adjustable parameters. The parameter η determines the stiffness at the hole perimeter and s determines the decay rate away from the hole. The function $\kappa(\rho)$ monotonically approaches unity as ρ increases.

For the spatial variation $E = E_\infty \exp[\eta\rho^s]$, the solutions p_1 and p_2 are known (Mohammadi and Dryden, 2009). They are given by

$$p_1(\rho) = \rho M\left(\frac{1-v_0}{s}, 1 + \frac{2}{s}, \eta\rho^s\right), \quad \text{and} \\ p_2(\rho) = \frac{1}{\rho} M\left(-\frac{1+v_0}{s}, 1 - \frac{2}{s}, \eta\rho^s\right), \quad (34)$$

where $M(a, b, x)$ is the Kummer's function and some of the basic properties of Kummer's function can be found in references (Abramowitz and Stegun, 1972; Erdelyi, 1981). Using Eqs. (31), (33) and (34), K_0 is written as

$$K_0 = 2 \exp(\eta) \Sigma_0, \quad (35)$$

where considering Eq. (33) the coefficient

$$\exp(\eta) = \frac{E_1}{E_\infty} \quad (36)$$

and the normalized stress concentration factor Σ_0 is given by

$$\Sigma_0 = \frac{1}{M\left(-\frac{1+v_0}{s}, 1 - \frac{2}{s}, \eta\right)}. \quad (37)$$

If this expression for Σ_0 is expanded as a power series in η it becomes clear that there are two limiting cases corresponding to small and large values for $|s|$

$$\Sigma_0 \sim \begin{cases} 1 & |s| \gg 1, \\ \exp[-(1+v_0)\eta/2] & |s| \ll 1. \end{cases} \quad (38)$$

For the case of homogeneous materials, $\eta = 0$, and the stress concentration factor reduces to the well-known result, (Pilkey and Pilkey, 2008), $K_0 = 2$.

5. Stress state due to pure shear loading: $m = 2$

Far field stresses $\sigma_y = \sigma_2$ and $\sigma_x = -\sigma_2$ are applied as shown in Fig. 1(b). The periphery of the hole is stress free. The stress function is then written as

$$\psi(\rho, \theta) = f(\rho) \cos(2\theta). \quad (39)$$

The problem is non-axisymmetric and the shear stress is not zero in this case. Assuming the functional form for $\kappa(\rho)$ proposed in Eq. (33), the governing differential Eq. (22) becomes

$$\rho^4 f'''' + 2[1 - sx]\rho^3 f''' - [9 - (v_0 - 1 - s)sx - s^2x^2]\rho^2 f'' \\ + [9 + (9 + v_0s - v_0)sx - v_0s^2x^2]\rho f' \\ + [4(v_0 - v_0s - 3)sx + 4v_0s^2x^2]f = 0. \quad (40)$$

The periphery of the hole is stress free so that, the boundary conditions are written as

$$\sigma_\rho(1) = 0, \quad \tau_{\rho\theta}(1) = 0, \quad \lim_{\rho \rightarrow \infty} \sigma_\rho \Big|_{\theta=0} = -\sigma_2. \quad (41)$$

Using Eqs. (13), (15) and (39), the boundary conditions in terms of $f(\rho)$ are

$$\lim_{\rho \rightarrow \infty} \left(\frac{f'(\rho)}{\rho} - \frac{4f(\rho)}{\rho^2} \right) = -\sigma_2, \quad (42)$$

$$f'(1) = 0, \quad (43)$$

$$f(1) = 0. \quad (44)$$

The independent solutions of governing Eq. (40) must be found and adjusted to fit the boundary conditions (42)–(44). After finding these solutions and applying the boundary conditions, the state of stress and consequently, the stress concentration factor can be determined.

5.1. Series solution

A closed form solution is not possible and here a series solution is used. The function $f(\rho)$ is written as a power series

$$f(\rho) = \rho^q \sum_{n=0}^{\infty} \mathcal{A}_n x^n, \quad (45)$$

where q is an unknown constant. Substituting Eq. (45) into the governing differential Eq. (40) leads to the recursion formula

$$\rho^q \sum_{n=0}^{\infty} \{ \alpha_n \mathcal{A}_n + \beta_{n-1} \mathcal{A}_{n-1} + \gamma_{n-2} \mathcal{A}_{n-2} \} x^n = 0, \quad (46)$$

where the coefficients $\mathcal{A}_{-1} = \mathcal{A}_{-2} \equiv 0$. The terms α_n , β_n , and γ_n are found as

$$\alpha_n = (q + ns - 4)(q + ns - 2)(q + ns)(q + ns + 2), \\ \beta_n = s(q + ns)[(q + ns - 1)\{-2(q + ns) + v_0 + 3 - s\} + 9 + v_0s - v_0] \\ + 4s(v_0 - v_0s - 3), \\ \gamma_n = s^2(q + ns)[q + ns - 1 - v_0] + 4s^2v_0. \quad (47)$$

Setting $n = 0$ in Eq. (46) yields $\alpha_0 \mathcal{A}_0 = 0$ and since $\mathcal{A}_0 \neq 0$ it follows that the indicial equation for q corresponds to

$$\alpha_0 = q(q - 4)(q - 2)(q + 2) = 0. \quad (48)$$

The indicial roots are then $q = (2, -2, 0, 4)$. An independent solution is associated with each root q of the indicial equation. For values of $n > 0$ the coefficients \mathcal{A}_n are deduced by the recursive relations

$$\alpha_1 \mathcal{A}_1 + \beta_0 \mathcal{A}_0 = 0, \quad n = 1, \\ \alpha_2 \mathcal{A}_2 + \beta_1 \mathcal{A}_1 + \gamma_0 \mathcal{A}_0 = 0, \quad n = 2, \\ \alpha_3 \mathcal{A}_3 + \beta_2 \mathcal{A}_2 + \gamma_1 \mathcal{A}_1 = 0, \quad n = 3, \quad (49)$$

⋮

$$\alpha_n \mathcal{A}_n + \beta_{n-1} \mathcal{A}_{n-1} + \gamma_{n-2} \mathcal{A}_{n-2} = 0,$$

where \mathcal{A}_0 is an arbitrary constant and the coefficients $\mathcal{A}_1, \mathcal{A}_2, \dots$ can be found as multiples of \mathcal{A}_0 . The solution corresponding to $q = 4$ gives unbounded stress as $\rho \rightarrow \infty$ and is not used here.

Now, the solutions corresponding to $q = (2, -2, 0)$ are calculated and the procedure is discussed. It is noted that, f_1 corresponds to $q = 2$; f_2 corresponds to $q = -2$; and f_3 corresponds to $q = 0$. Here, using the recursive formula (46) and (49), the three solutions of the governing differential Eq. (40) when $m = 2$ are determined.

5.2. Solution corresponding to uniform far-field stress

Consider $f_1(\rho)$ as the first general solution corresponding to $q = 2$. This solution refers to uniform far-field stress and using Eq. (45), it is written as

$$f_1(\rho) = \frac{\rho^2}{2} \sum_{n=0}^{\infty} F_n x^n, \quad (50)$$

where the coefficients F_n are defined from

$$\begin{aligned}
\alpha_1 F_1 + \beta_0 F_0 &= 0, \quad n = 1, \\
\alpha_2 F_2 + \beta_1 F_1 + \gamma_0 F_0 &= 0, \quad n = 2, \\
\alpha_3 F_3 + \beta_2 F_2 + \gamma_1 F_1 &= 0, \quad n = 3, \\
&\vdots \\
\alpha_n F_n + \beta_{n-1} F_{n-1} + \gamma_{n-2} F_{n-2} &= 0,
\end{aligned} \quad (51)$$

where the coefficients α_n , β_n , and γ_n are

$$\begin{aligned}
\alpha_n &= ns(ns + 4)(ns - 2)(ns + 2), \\
\beta_n &= s(2 + ns)[(1 + ns)\{-2ns + v_0 - 1 - s\} + 9 + v_0 s - v_0] \\
&\quad + 4s(v_0 - v_0 s - 3), \\
\gamma_n &= s^2(2 + ns)[ns + 1 - v_0] + 4s^2 v_0.
\end{aligned} \quad (52)$$

The coefficients

$$\begin{aligned}
F_1 &= \left[\frac{2(1 + v_0)}{(s + 4)(s + 2)} \right] F_0, \\
F_2 &= \left[\frac{(1 + v_0)(2s^2 + s^3 - 2 - v_0 s^2 - 2v_0 - 4s)}{4(s + 4)(s + 2)^2(s + 1)(s - 1)} \right] F_0
\end{aligned} \quad (53)$$

are the first two terms of the series (50) and F_0 is an arbitrary constant. For the sake of brevity, the other coefficients are not given. In addition the coefficient F_0 is arbitrary and is considered as $F_0 = 1$.

5.3. Solution associated with $q = -2$

The solution $f_2(\rho)$ corresponds to the root $q = -2$ and is written as

$$f_2(\rho) = \frac{1}{2\rho^2} \sum_{n=0}^{\infty} G_n \rho^n, \quad (54)$$

where the coefficients G_n are defined from

$$\begin{aligned}
\alpha_1 G_1 + \beta_0 G_0 &= 0, \quad n = 1, \\
\alpha_2 G_2 + \beta_1 G_1 + \gamma_0 G_0 &= 0, \quad n = 2, \\
\alpha_3 G_3 + \beta_2 G_2 + \gamma_1 G_1 &= 0, \quad n = 3, \\
&\vdots \\
\alpha_n G_n + \beta_{n-1} G_{n-1} + \gamma_{n-2} G_{n-2} &= 0,
\end{aligned} \quad (55)$$

where the coefficients α_n , β_n , and γ_n are

$$\begin{aligned}
\alpha_n &= ns(ns - 6)(ns - 4)(ns - 2), \\
\beta_n &= s(ns - 2)[(ns - 3)\{-2ns + v_0 + 7 - s\} + 9 + v_0 s - v_0] \\
&\quad + 4s(v_0 - v_0 s - 3), \\
\gamma_n &= s^2(ns - 2)[ns - 3 - v_0] + 4s^2 v_0.
\end{aligned} \quad (56)$$

The first two coefficients of the series (54) are then written as

$$\begin{aligned}
G_1 &= \left[\frac{6(1 + v_0)}{(s - 4)(s - 6)} \right] G_0, \\
G_2 &= \left[\frac{3(1 + v_0)(10s + 6v_0 s + s^3 - 6 - 6v_0 - 6s^2 - v_0 s^2)}{4(s - 4)(s - 6)(s - 3)(s - 2)(s - 1)} \right] G_0
\end{aligned} \quad (57)$$

and the coefficient $G_0 = 1$.

5.4. Solution associated with $q = 0$

The third solution $f_3(\rho)$, corresponds to the root $q = 0$ and is written as

$$f_3(\rho) = \sum_{n=0}^{\infty} H_n \rho^n, \quad (58)$$

where the coefficients H_n are defined from

$$\begin{aligned}
\alpha_1 H_1 + \beta_0 H_0 &= 0, \quad n = 1, \\
\alpha_2 H_2 + \beta_1 H_1 + \gamma_0 H_0 &= 0, \quad n = 2, \\
\alpha_3 H_3 + \beta_2 H_2 + \gamma_1 H_1 &= 0, \quad n = 3, \\
&\vdots \\
\alpha_n H_n + \beta_{n-1} H_{n-1} + \gamma_{n-2} H_{n-2} &= 0,
\end{aligned} \quad (59)$$

where the coefficients α_n , β_n , and γ_n are

$$\begin{aligned}
\alpha_n &= ns(ns - 4)(ns - 2)(ns + 2), \\
\beta_n &= ns^2[(ns - 1)\{-2ns + v_0 + 3 - s\} + 9 + v_0 s - v_0] \\
&\quad + 4s(v_0 - v_0 s - 3), \\
\gamma_n &= ns^3[ns - 1 - v_0] + 4s^2 v_0.
\end{aligned} \quad (60)$$

The first two coefficients are then written as

$$\begin{aligned}
H_1 &= \left[\frac{4(v_0 s + 3 - v_0)}{(s - 4)(s - 2)(s + 2)} \right] H_0, \\
H_2 &= \left[\frac{2s^3 v_0 - v_0 s^2 - 2v_0^2 s^2 + 9s^2 - 4v_0 s + 4v_0^2 s - 2v_0^2 + 12v_0 - 18}{4(s - 4)(s - 2)(s - 1)(s + 1)(s + 2)} \right] H_0.
\end{aligned} \quad (61)$$

Like previous solutions, the coefficient $H_0 = 1$.

5.5. The stress function $f(\rho)$ and stress concentration factor K_2

Considering the boundary conditions (42)–(44) and using the three solutions defined in (50), (54) and (58), the stress function can be determined and it is written as

$$f(\rho) = \sigma_2 \left(\frac{[f_2 f'_3 - f_3 f'_2]_1 f_1(\rho) + [f_3 f'_1 - f_1 f'_3]_1 f_2(\rho) + [f_1 f'_2 - f_2 f'_1]_1 f_3(\rho)}{[f_2 f'_3 - f_3 f'_2]_1} \right), \quad (62)$$

where the terms $[\dots]_1$ indicate evaluation at $\rho = 1$. Far from the hole, when $\rho \gg 1$, the stress function $f \sim \sigma_2 \rho^2 / 2$ corresponding to uniform far-field stress. Here, the stress function $f(\rho)$ is approximated by a truncated series containing terms up to η^N .

The hoop stress is given by $\sigma_\theta = f''(\rho) \cos(2\theta)$ and attains its maximum value at $\theta = 0$ on the periphery of the hole; thus, the stress concentration factor for the pure shear case, i.e. $m = 2$, is written as

$$K_2 = \left[\frac{(f_2 f'_3 - f_3 f'_2) f''_1 + (f_3 f'_1 - f_1 f'_3) f''_2 - (f_2 f'_1 - f_1 f'_2) f''_3}{f_2 f'_3 - f_3 f'_2} \right]_1. \quad (63)$$

In the same vein as Eq. (35), K_2 is written as

$$K_2 = 4 \left(\frac{E_1}{E_\infty} \right) \Sigma_2, \quad (64)$$

where the normalized stress concentration factor Σ_2 is given by

$$\Sigma_2 = 1 + a_1 \eta + \frac{a_2 \eta^2}{2!} + \frac{a_3 \eta^3}{3!} + \dots + \frac{a_N \eta^N}{N!}, \quad (65)$$

where the coefficients a_1, \dots are known and they are functions of v_0 and s . Upon inspection of the series terms, two limiting cases, corresponding to small and large values for $|s|$, are observed to be given by

$$\Sigma_2 \sim \begin{cases} 1 & |s| \gg 1, \\ \exp[(v_0 - 3)\eta/4] & |s| \ll 1. \end{cases} \quad (66)$$

For the case of homogeneous materials, $\eta = 0$, and the stress concentration factor reduces to the well-known result, (Pilkey and Pilkey, 2008), $K_2 = 4$.

6. Results and discussion

Suppose that the plate is subjected to uniform far-field stress with components σ_x and σ_y . By inspection of Fig. 1(a) and (b), it is clear that $\sigma_x = \sigma_0 - \sigma_2$ and $\sigma_y = \sigma_0 + \sigma_2$. It then follows that

$$\sigma_0 = \frac{\sigma_y + \sigma_x}{2}, \quad \text{and} \quad \sigma_2 = \frac{\sigma_y - \sigma_x}{2}. \quad (67)$$

For uniaxial tension, $\sigma_x = 0$ and the stress concentration factor is then

$$K = \left(\frac{E_1}{E_\infty} \right) (\Sigma_0 + 2\Sigma_2). \quad (68)$$

When $\eta = 0$ this reduces to the well-known result $K = 3$.

Here, the elastic stiffness is given by $E = E_\infty \exp(\eta \rho^s)$ where $s < 0$. The far-field stiffness, $E = E_\infty$, is attained when $\rho^s \approx 0$. The requirement for ρ^s to become arbitrarily small can be written as $(1+t)^s = e^m$ where $m < 0$. Upon solving for t , it is found that

$$t = e^{\frac{m}{s}} - 1 = \frac{m}{s} + \frac{1}{2} \left(\frac{m}{s} \right)^2 + \frac{1}{3!} \left(\frac{m}{s} \right)^3 + \dots \quad (69)$$

The convergence of this estimate for t depends on the ratio m/s . For simplicity $m = -1$ and t is estimated as

$$t = -\frac{1}{s}. \quad (70)$$

This gives a characteristic parameter to estimate the width of the inhomogeneous zone surrounding the hole and it is similar to the use of a characteristic time in electrical engineering. Fig. 2 shows the distribution of $\ln E/E_\infty$ versus the dimensionless radius ρ for different values of η and t .

This section is divided into two parts. First, Poisson's ratio is considered as constant and the effect of nonhomogeneous stiffness on the stress concentration factors is discussed. Secondly, Young's modulus is held constant and the influence of varying Poisson's ratio is analyzed.

6.1. Effect of nonhomogeneous stiffness upon K_0

For biaxial loading the stress concentration factor is $K_0 = 2(E_1/E_\infty)\Sigma_0$ where the function Σ_0 is given in Eq. (37)

$$\Sigma_0 = \frac{1}{M(t + tv_0, 1 + 2t, \eta)}, \quad (71)$$

where $M(a, b, x)$ is the Kummer's function. When $t = 0$ the function $\Sigma_0 = 1$ and its derivative is given by

$$\left. \frac{\partial \Sigma_0}{\partial t} \right|_0 = -(1 + v_0) \left(\eta + \frac{\eta^2}{2 \times 2!} + \frac{\eta^3}{3 \times 3!} + \frac{\eta^4}{4 \times 4!} + \dots \right). \quad (72)$$

When $t \gg 1$ the function Σ_0 approaches the limit $L_0 = \exp[-(1 + v_0)\eta/2]$ as given in Eq. (38). Fig. 3 shows a graph of $\ln \Sigma_0$ versus t for various values of η and Poisson's ratio $v = v_0 = 1/4$. As t

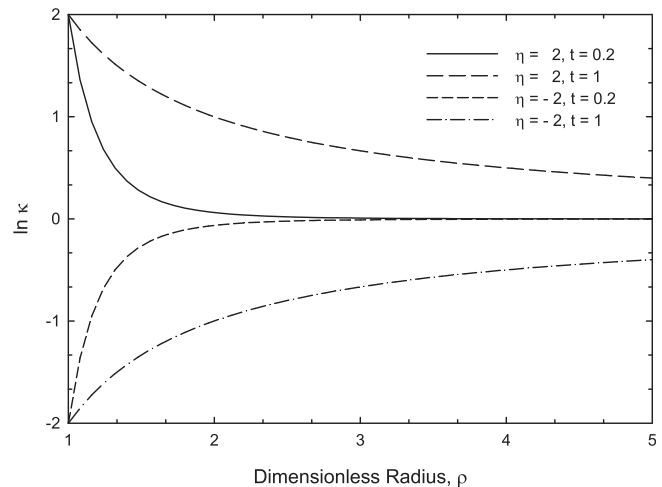


Fig. 2. Graph of normalized Young's modulus $\ln \kappa(\rho)$, defined in Eq. (33), versus dimensionless radius ρ for the values of η and t shown.

becomes large, $\ln \Sigma_0 \sim \pm 5\eta/8$. The most rapid change in Σ_0 occurs in the region $0 < t < 1$ and a Taylor's expansion around $t = 0$ requires too many terms to be very useful. However, commonly available software packages such as MAPLE allow convenient evaluation of the Kummer's function. The behavior of K_0 for other values of v_0 is similar.

6.2. Effect of nonhomogeneous stiffness upon K_2

For the case of pure shear, the stress concentration factor is $K_2 = 4(E_1/E_\infty)\Sigma_2$ where the function Σ_2 is given in Eq. (65)

$$\Sigma_2 = 1 + a_1\eta + \frac{a_2\eta^2}{2!} + \frac{a_3\eta^3}{3!} + \frac{a_4\eta^4}{4!} + \frac{a_5\eta^5}{5!}.$$

The number of terms required for the series to converge evidently depends upon the magnitude of η and as might be expected, the terms get more complicated as N becomes large. Moving into the plate, from the far field to the periphery of the hole, the stiffness changes by a factor $\exp(\eta)$. In most FGMs this change is not exceedingly large and the value of η is likely less than 2. For this value of η the series gives a reasonable estimate if it is truncated when $N = 5$. The coefficients a_1, a_2, \dots, a_5 depend on $t = -1/s$ and v_0 . The coefficient $a_1 = (b_{10} + b_{11}v_0)/c_1$ and is written as

$$a_1 = \frac{-3t - 12t^2 - 36t^3}{1 + 12t + 44t^2 + 48t^3} + \frac{v_0(-t + 8t^2 + 12t^3)}{1 + 12t + 44t^2 + 48t^3}. \quad (73)$$

The second coefficient has the form $a_2 = (b_{20} + b_{21}v_0 + b_{22}v_0^2)/c_2$ and is written as Subsequent coefficients have the form $a_n = (b_{n0} + b_{n1}v_0 + \dots + b_{nn}v_0^n)/C_n$ but become too unwieldy to be useful and they are not presented.

When $t = 0$ the function $\Sigma_2 = 1$ and its derivative is given by

$$\begin{aligned} \frac{b_{20}}{c_2} &= \frac{-3t - 27t^2 - 81t^3 + 180t^4 + 1938t^5 + 7128t^6 + 13608t^7 + 7776t^8}{2 + 56t + 662t^2 + 4304t^3 + 16784t^4 + 40064t^5 + 56928t^6 + 43776t^7 + 13824t^8}, \\ \frac{b_{21}}{c_2} &= \frac{-t + 14t^2 + 115t^3 + 112t^4 - 2544t^5 - 11088t^6 - 14256t^7 - 5184t^8}{2 + 56t + 662t^2 + 4304t^3 + 16784t^4 + 40064t^5 + 56928t^6 + 43776t^7 + 13824t^8}, \\ \frac{b_{22}}{c_2} &= \frac{3t^2 - 28t^3 - 68t^4 + 542t^5 + 1848t^6 + 2088t^7 + 864t^8}{2 + 56t + 662t^2 + 4304t^3 + 16784t^4 + 40064t^5 + 56928t^6 + 43776t^7 + 13824t^8}. \end{aligned} \quad (74)$$

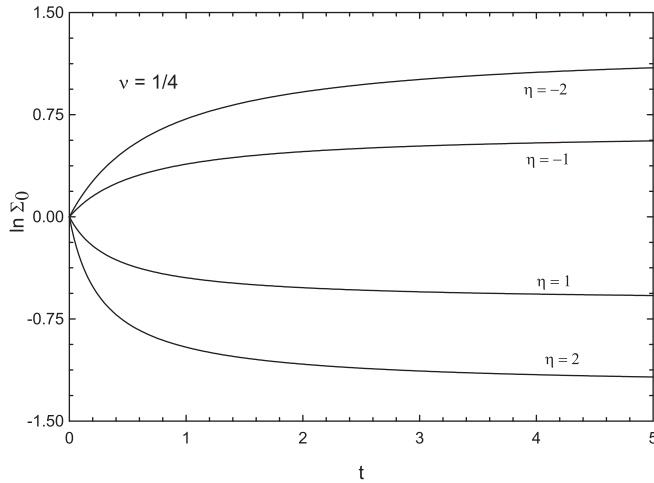


Fig. 3. Graph of $\ln \Sigma_0$ versus t for the values of η shown and Poisson's ratio $\nu_0 = 1/4$. At $t = 0$ the slope is given by Eq. (72). For large values of t the limiting values $\pm 5\eta/8$ are attained.

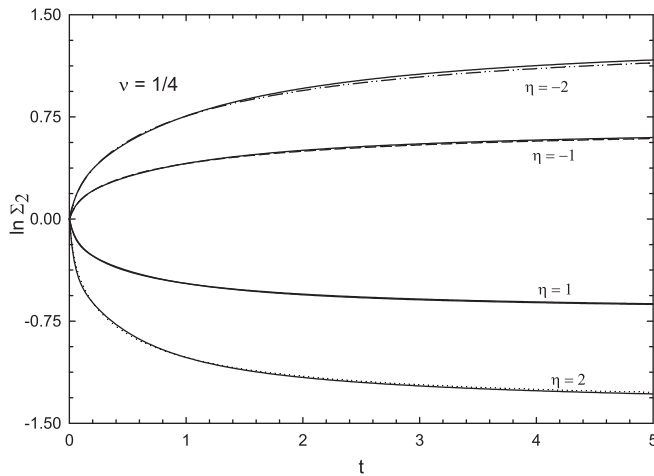


Fig. 4. Graph of $\ln \Sigma_2$ versus t for the values of η shown and Poisson's ratio $\nu_0 = 1/4$. At $t = 0$ the slope is equal to ϑ which is given by Eq. (75). For large values of t the limiting values $\pm 11\eta/16$ are attained. The solid lines represent the series solution and the dashed lines are obtained from approximation given in Eq. (76).

$$\vartheta \equiv \left. \frac{\partial \Sigma_2}{\partial t} \right|_0 = -(3 + \nu_0) \left(\eta + \frac{\eta^2}{2 \times 2!} + \frac{\eta^3}{3 \times 3!} + \frac{\eta^4}{4 \times 4!} + \dots \right). \quad (75)$$

When $t \gg 1$ the function Σ_2 approaches the limit $L_2 = \exp[(\nu_0 - 3)\eta/4]$ as given in Eq. (66). Fig. 4 shows a graph of $\ln \Sigma_2$ versus t for various values of η and Poisson's ratio $\nu = \nu_0 = 1/4$. The solid lines in Fig. 4 represent the series solution and the dashed lines are found from an approximate method which is described later. The most rapid change in Σ_2 occurs in the region $0 < t < 1$ and a Taylor's expansion around $t = 0$ requires too many terms to be very useful. As t becomes large, $\ln \Sigma_2 \sim \pm 11\eta/16$. The behavior of Σ_2 is qualitatively similar to that of Σ_0 . However, unlike Σ_0 , the series terms in the expression for Σ_2 can only be found after the lengthy calculation.

6.2.1. Approximate solution

To avoid the long calculation to find the coefficients, a_1 to a_5 , a method of fitting the rational form

$$S = 1 + \frac{\vartheta t + (L_2 - 1)w_1 t^2}{1 + w_2 t + w_1 t^2}, \quad (76)$$

to the exact result is presented. At $t = 0$ this approximate form agrees with Σ_2 and its derivative. At the other extreme when $t \rightarrow \infty$, the approximate form S approaches the limit L_2 . The parameters w_1 and w_2 are adjusted to render a reasonable approximation and this is accomplished by interpolating the expression for S through two suitably chosen points $[t_1, S_1]$ and $[t_2, S_2]$. At these two interpolation points $S = \Sigma_2$. By trial and error, it has been found that setting $t_1 = 1/5$ and $t_2 = 1$ produces an expression S with a relative error $(\Sigma_2 - S)/\Sigma_2 < 0.05$. After some algebra it is found that the parameter w_1 is

$$w_1 = (1 - 2\nu_0)(1 - 4\nu_0)(14.55\delta_0 + 28.83\delta_1 + 8.354\delta_{-1} + 69.64\delta_2 + 5.486\delta_{-2}) + 8\nu_0(1 - 2\nu_0)(12.92\delta_0 + 27.45\delta_1 + 6.816\delta_{-1} + 72.44\delta_2 + 3.986\delta_{-2}) + 2\nu_0(4\nu_0 - 1)(11.00\delta_0 + 25.30\delta_1 + 5.453\delta_{-1} + 73.87\delta_2 + 2.989\delta_{-2})$$

and w_2 is given by

$$w_2 = (1 - 2\nu_0)(1 - 4\nu_0)(13.09\delta_0 + 17.65\delta_1 + 11.05\delta_{-1} + 27.04\delta_2 + 10.78\delta_{-2}) + 8\nu_0(1 - 2\nu_0)(13.62\delta_0 + 19.17\delta_1 + 10.66\delta_{-1} + 30.01\delta_2 + 9.250\delta_{-2}) + 2\nu_0(4\nu_0 - 1)(14.25\delta_0 + 20.48\delta_1 + 10.79\delta_{-1} + 32.99\delta_2 + 8.852\delta_{-2}).$$

The Lagrangian interpolation functions are,

$$\begin{aligned} \delta_0 &= (1 - \eta^2)(4 - \eta^2)/4, \\ \delta_1 &= (1 + \eta)(4 - \eta^2)\eta/6, \\ \delta_{-1} &= (\eta - 1)(4 - \eta^2)\eta/6, \\ \delta_2 &= (\eta + 2)(\eta^2 - 1)\eta/24, \\ \delta_{-2} &= (\eta - 2)(\eta^2 - 1)\eta/24. \end{aligned} \quad (77)$$

For example if $\nu_0 = 1/4$ and $\eta = 1$, then $L_2 \approx .5028$, $\vartheta \approx -4.282$, $w_1 \approx 27.45$, and $w_2 \approx 19.17$. The approximation S is then found to be

$$S = 1.0 + \frac{-4.282t - 13.65t^2}{1.0 + 19.17t + 27.45t^2}$$

and as shown in Fig. 4 this gives a reasonably accurate approximation.

6.3. Influence of varying Poisson's ratio upon K_0

The goal here is to find the effect of varying Poisson's ratio upon the stress concentration factors when Young's modulus is almost constant. Letting η approach zero corresponds to constant stiffness and it is desired that ν change from ν_1 to ν_∞ as the radius increases. Poisson's ratio is given in Eq. (2) and as $\eta \rightarrow 0$, the function $\kappa \approx 1 + \eta\rho^s$. Poisson's ratio is then given by $\nu = \nu_\infty + (\nu_1 - \nu_\infty)\rho^s$ and the coefficient ν_0 is given by

$$\nu_0 \approx \frac{\omega}{\eta}, \quad (78)$$

where $\omega = \nu_\infty - \nu_1$. Using Eq. (78) and as η approaches zero,

$$\Sigma_0 = \frac{1}{M(t(1 + \nu_0), 1 + 2t, \eta)} \rightarrow \frac{1}{{}_0F_1(1 + 2t, \omega t)}, \quad (79)$$

where ${}_0F_1(a, x)$ is the Hypergeometric function and some of its basic properties can be found in references (Abramowitz and Stegun, 1972; Erdelyi, 1981). For the case of homogeneous materials, i.e. $\omega = 0$, the coefficient $\Sigma_0 = 1$ and $K_0 = 2$. Fig. 5 shows the distribution of $\ln \Sigma_0$ versus t for various values of ω . For the maximum change in Poisson's ratio, i.e. $|\omega| = 0.5$, it is found that as t becomes large K_0 changes by 28% from the case where Poisson's ratio is constant.

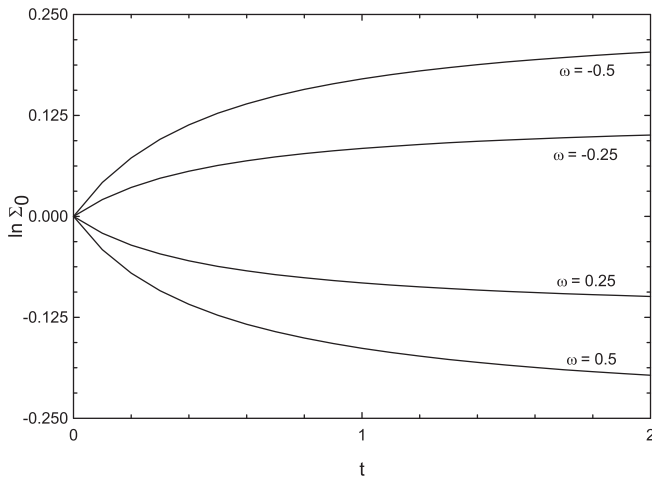


Fig. 5. Graph of $\ln \Sigma_0$ versus t for the values of ω shown. The coefficient $\eta \rightarrow 0$ and Young's modulus is virtually constant; nonetheless, Poisson's ratio varies between ν_1 and ν_∞ . The stress concentration factor differs by 28% from the case where Poisson's ratio is constant.

6.4. Influence of varying Poisson's ratio upon K_2

Considering $\eta \rightarrow 0$, performing the same limiting process, and using Eq. (78), the governing differential Eq. (40) for the case of almost constant Young's modulus is written as

$$\rho^4 f'''' + 2\rho^3 f''' - [9 - \omega s \rho^s] \rho^2 f'' + [9 + \omega s(s-1)\rho^s] \rho f' + [4\omega s(1-s)\rho^s] f = 0. \quad (80)$$

As mentioned before, only three linearly independent solutions of Eq. (80) yield bounded stresses when $\rho \rightarrow \infty$ and they are written as

$$f_1(\rho) = \frac{\rho^2}{2} {}_2F_3\left(\frac{1}{2} - t + \frac{\zeta}{2}, \frac{1}{2} - t - \frac{\zeta}{2}; 1 - 2t, 1 + 2t, 1 - 4t; \omega t \rho^s\right), \quad (81)$$

$$f_2(\rho) = \frac{1}{2\rho^2} {}_2F_3\left(\frac{1}{2} + 3t + \frac{\zeta}{2}, \frac{1}{2} + 3t - \frac{\zeta}{2}; 1 + 4t, 1 + 2t, 1 + 6t; \omega t \rho^s\right), \quad (82)$$

$$f_3(\rho) = {}_2F_3\left(\frac{1}{2} + t + \frac{\zeta}{2}, \frac{1}{2} + t - \frac{\zeta}{2}; 1 - 2t, 1 + 2t, 1 + 4t; \omega t \rho^s\right), \quad (83)$$

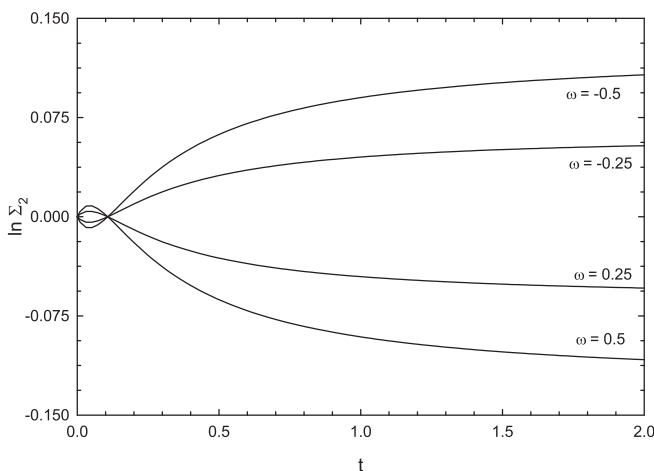


Fig. 6. Graph of $\ln \Sigma_2$ versus t for the values of ω shown. The coefficient $\eta \rightarrow 0$ and Young's modulus is virtually constant; nonetheless, Poisson's ratio varies between ν_1 and ν_∞ . The stress concentration factor differs by 13% from the case where Poisson's ratio is constant.

where the coefficient

$$\zeta = \sqrt{1 - 12t - 12t^2}, \quad (84)$$

and ${}_2F_3(a, b; c, d, e; x)$ is the Hypergeometric function; some of its basic properties can be found in references (Abramowitz and Stegun, 1972; Erdelyi, 1981). Using Eqs. (63) and (64), the normalized stress concentration factor Σ_2 is calculated. Fig. 6 shows the distribution of $\ln \Sigma_2$ versus t for different values of ω . For the case of homogeneous materials, i.e. $\omega = 0$, the coefficient $\Sigma_2 = 1$ and $K_2 = 4$. It is noted that for the maximum change in Poisson's ratio, as t becomes large K_2 changes by 13% from the case where Poisson's ratio is constant.

7. Concluding remarks

In this paper the stress concentration factor around a circular hole in a radially inhomogeneous plate subjected to uniform biaxial tension and pure shear loading has been considered. An exponential function has been used to model the spatial variation of the elastic properties. The parameters η and s can be adjusted so that the shape of this function is reasonably general.

An analytical expression (31) for the stress concentration factor K_0 , i.e. uniform biaxial tension, was calculated. The normalized stress concentration factor Σ_0 was presented in terms of Kummer's function. The two Kummer's functions are given in Eq. (34). If $t = -1/s$, then it appears that the values $t = (1 + N)/2$ where N is an integer is not possible; otherwise the function $p_1(\rho)$ is not defined. However, because K_0 depends on the Wronskian, these forbidden values of t are not problematic. A similar phenomenon occurs when K_2 is calculated.

Poisson's ratio was considered as constant and the effect of non-homogeneous stiffness was considered on K_0 and K_2 . Since K_2 did not have a closed form solution, a reasonable approximation in the range $|\eta| < 2$ was devised. Subsequently, Young's modulus was considered virtually constant and a limiting process was performed. It was concluded that for the maximum change in Poisson's ratio, as t becomes large K_0 and K_2 change by 28% and 13%, respectively from the case where Poisson's ratio is constant.

Acknowledgment

The authors are grateful for the funding provided by NSERC.

References

- Abramowitz, M., Stegun, I.A., 1972. Handbook of Mathematical Functions. Dover Publications, New York.
- Batra, R.C., Nie, G.J., 2009. Analytical solutions for functionally graded incompressible eccentric and non-axisymmetrically loaded circular cylinders. Compos. Struct. doi:10.1016/j.compstruct.2009.10.022.
- Braun, M., 1993. Differential Equations and Their Applications, fourth ed. Springer, New York.
- Dryden, J., Jayaraman, K., 2006. Effect of inhomogeneity on the stress in pipes. J. Elasticity 83, 179–189.
- Dryden, J.R., 2007. Bending of inhomogeneous curved bars. Int. J. Solids. Struct. 44, 4158–4166.
- Erdelyi, A., 1981. Higher Transcendental Functions, vol. 1. Robert E. Krieger Publishing Company, Malabar, Florida.
- Fukui, Y., Okada, H., Kumazawa, N., Watanabe, Y., Yamanaka, N., Oya-Seimiya, Y., 1999. Manufacturing of Al–Al₃Fe functionally graded material using the vacuum centrifugal method and measurements of its mechanical properties. J. Jpn. Inst. Light Met. 49, 35–40.
- Horgan, C.O., Chan, A.M., 1999. The pressurized hollow cylinder or disk problem for functionally graded isotropic linearly elastic materials. J. Elasticity 55, 43–59.
- Islam, M.U., 1996. An overview of research in the fields of laser surface modification and laser machining at the integrated manufacturing technologies institute NRC. Adv. Perform. Mater. 3, 215–238.
- Jabbari, M., Sohrabpour, S., Eslami, M.R., 2002. Mechanical and thermal stresses in a functionally graded hollow cylinder due to radially symmetric loads. Int. J. Pres. Ves. Pip. 79, 493–497.

- Jabbari, M., Sohrabpour, S., Eslami, M.R., 2003. General solutions for mechanical and thermal stresses in a functionally graded hollow cylinder due to nonaxisymmetric steady-state loads. *J. Appl. Mech.-T. ASME*, 70, 111–118.
- Kardomateas, G.A., 1990. Bending of a cylindrically orthotropic curved beam with linearly distributed elastic constants. *Q. J. Mech. Appl. Math.* 43, 43–56.
- Koizumi, M., 1997. FGM activities in Japan. *Compos. Part B* 28B, 1–4.
- Kubair, D.V., Bhanu-Chandar, B., 2008. Stress concentration factor due to a circular hole in functionally graded panels under uniaxial tension. *Int. J. Mech. Sci.* 50, 732–742.
- Lekhnitskii, S.G., 1981. *Theory of Elasticity of an Anisotropic Body*. Mir Publishers, Moscow.
- Love, A.E.H., 1906. *A Treatise on the Mathematical Theory of Elasticity*, second ed. Cambridge University Press, Warehouse.
- Lutz, M.P., Zimmerman, R.W., 1996a. Thermal stresses and effective thermal expansion coefficient of a functionally gradient sphere. *J. Therm. Stresses* 19, 39–54.
- Lutz, M.P., Zimmerman, R.W., 1996b. Effect of the interphase zone on the bulk modulus of a particulate composite. *J. Appl. Mech.* 63, 855–861.
- Markworth, A.J., Ramesh, K.S., Parks, W.P., 1995. Modelling studies applied to functionally graded materials. *J. Mater. Sci.* 30, 2183–2193.
- Miyamoto, Y., Kaysser, W.A., Rabin, R.H., Kawasaki, A., Ford, R.G., 1999. *Functionally Graded Materials: Design Processing and Applications*. Kluwer Academic Publishers, USA.
- Mohammadi, M., Dryden, J.R., 2008. Thermal stresses in a nonhomogeneous curved beam. *J. Therm. Stresses* 31, 587–598.
- Mohammadi, M., Dryden, J.R., 2009. Influence of the spatial variation of Poisson's ratio upon the elastic field in nonhomogeneous axisymmetric bodies. *Int. J. Solids. Struct.* 46, 225–232.
- Nie, G.J., Batra, R.C., 2009. Static deformations of functionally graded polar-orthotropic cylinders with elliptical inner and circular outer surfaces. *Compos. Sci. Technol.* doi:10.1016/j.compscitech.2009.11.018.
- Noda, N., 1999. Thermal stresses in functionally graded materials. *J. Therm. Stresses* 22, 477–512.
- Pilkey, W.D., Pilkey, D.F., 2008. *Peterson's Stress Concentration Factors*, third ed. John Wiley and Sons, Hoboken, New Jersey.
- Poultangari, R., Jabbari, M., Eslami, M.R., 2008. Functionally graded hollow spheres under non-axisymmetric thermo-mechanical loads. *Int. J. Pres. Ves. Pip.* 85, 295–305.
- Savin, G.N., 1961. *Stress Concentration around Holes*, International Series of Monographs in Aeronautics and Astronautics. Pergamon Press, New York.
- Shao, Z.S., Ang, K.K., Reddy, J.N., Wang, T.J., 2008. Nonaxisymmetric thermomechanical analysis of functionally graded hollow cylinders. *J. Therm. Stresses* 31, 515–536.
- Simonet, J., Kapelski, G., Bouvard, D., 2007. A sedimentation process for the fabrication of solid oxide fuel cell cathodes with graded composition. *J. Eur. Ceram. Soc.* 27, 3113–3116.
- Timoshenko, S., Goodier, J.N., 1970. *Theory of Elasticity*, third ed. McGraw-Hill, New York.
- Tutuncu, N., 2007. Stresses in thick-walled FGM cylinders with exponentially-varying properties. *Eng. Struct.* 29, 2032–2035.
- Wang, C., 1953. *Applied Elasticity*. McGraw-Hill, New York.
- Watari, F., Yokoyama, A., Saso, F., Uo, M., Kawasaki, T., 1997. Fabrication and properties of functionally graded dental implant. *Compos. Part B* 28, 5–11.
- Yang, Q., Gao, C.-F., Chen, W., 2009. Stress analysis of a functional graded material plate with a circular hole. *Arch. Appl. Mech.* doi:10.1007/s00419-009-0349-3.
- Zimmerman, R.W., Lutz, M.P., 1999. Thermal stresses and thermal expansion in a uniformly heated functionally graded cylinder. *J. Therm. Stresses* 22, 177–188.